

Supplementary Materials for

The unfolded protein response regulator ATF6 promotes mesodermal differentiation

Heike Kroeger, Neil Grimsey, Ryan Paxman, Wei-Chieh Chiang, Lars Plate, Ying Jones, Peter X. Shaw, JoAnn Trejo, Stephen H. Tsang, Evan Powers, Jeffery W. Kelly, R. Luke Wiseman, Jonathan H. Lin*

*Corresponding author. Email: jlin@ucsd.edu

Published 13 February 2018, *Sci. Signal.* **11**, eaan5785 (2018)

DOI: 10.1126/scisignal.aan5785

The PDF file includes:

Fig. S1. AA147 significantly increases ATF6(N) and GRP78/BiP protein abundance.

Fig. S2. AA147 treatment does not affect Wnt, DNA regulation, mRNA surveillance, Fanconi anemia, and cell death signaling pathways in stem cells.

Fig. S3. AA147 treatment does not induce mesodermal marker genes in HEK293 cells.

Legends for tables S1 to S3

Table S4. RNA-seq data set in our transcriptome database.

Other Supplementary Material for this manuscript includes the following:

(available at www.sciencesignaling.org/cgi/content/full/11/517/eaan5785/DC1)

Table S1 (Microsoft Excel format). Summary of genes used in volcano plots.

Table S2 (Microsoft Excel format). Raw RNA-seq data.

Table S3 (Microsoft Excel format). Comparison study using other cell types and tissues.

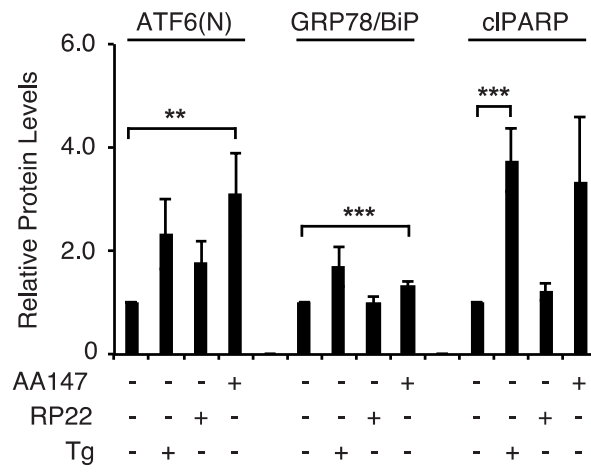


Figure S1. AA147 significantly increases ATF6(N) and GRP78/BiP protein abundance. Quantification of Western blot data provided in Figure 1C. AA147 (15 μ M) was used to activate ATF6 in stem cells during a short exposure of 4 hours. The analogue RP22 was used under similar conditions. Thapsigargin (Tg), positive control for ATF6 activation. Data were analyzed relative to untreated samples, and are means \pm SD from 4 experiments. **P<0.05, ***P< 0.005.

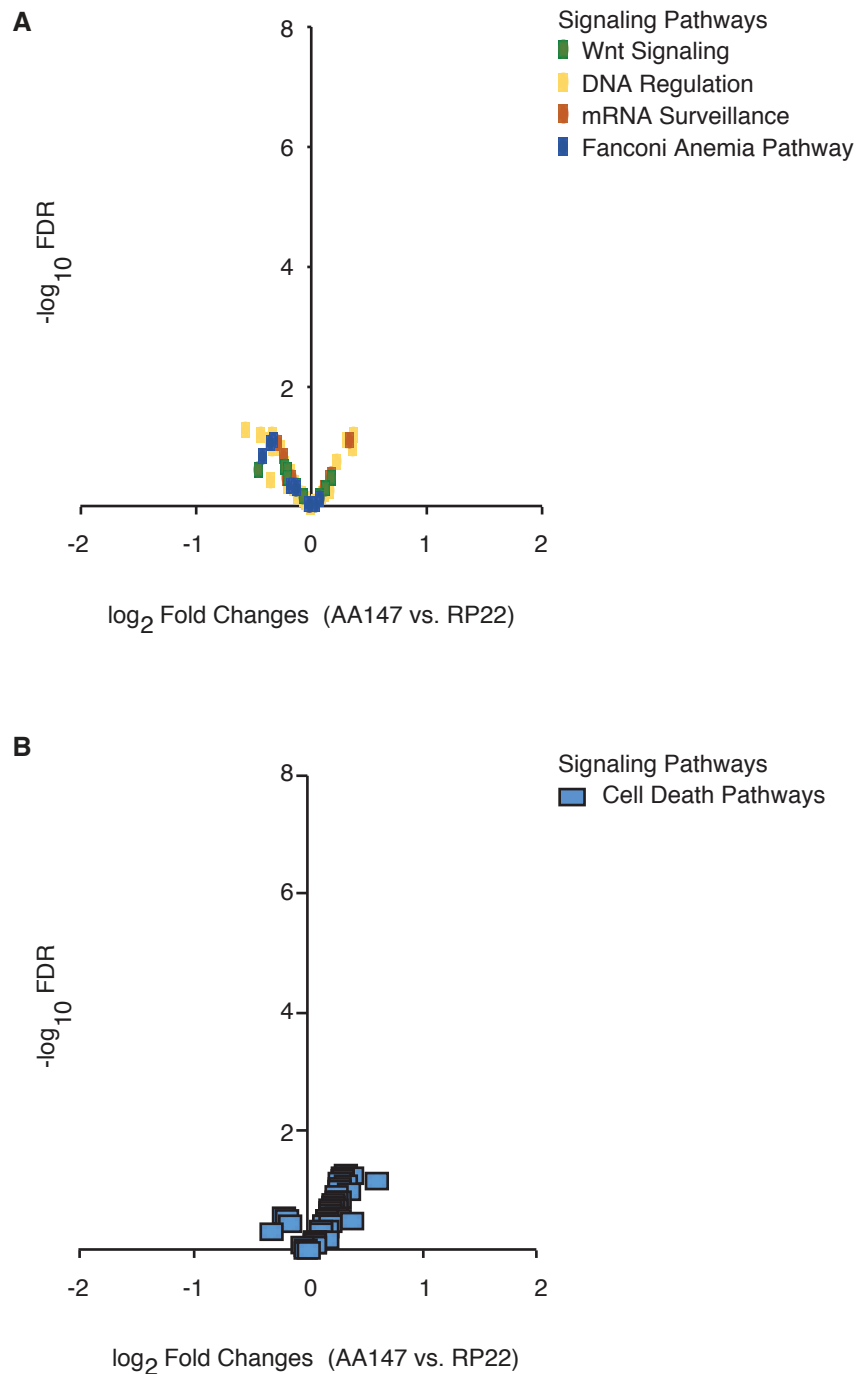


Figure S2. AA147 treatment does not affect Wnt, DNA regulation, mRNA surveillance, Fanconi anemia, and cell death signaling pathways in stem cells. Volcano plot representation of RNA-Seq data of AA147-treated hESCs relative to RP22-treated hESCs. Colored circles represent transcriptional target genes associated with indicated signaling pathways. \log_2 fold changes in mRNA levels collected by RNA-Seq are plotted on the x -axis. $-\log_{10}$ fold false discovery rate (FDR) values of RNA-Seq data are plotted on the y -axis. AA147 (10 μM) - and RP22 (10 μM)-treated samples were quantified relative to day 1, and AA147 levels are shown normalized to RP22 at day 13.

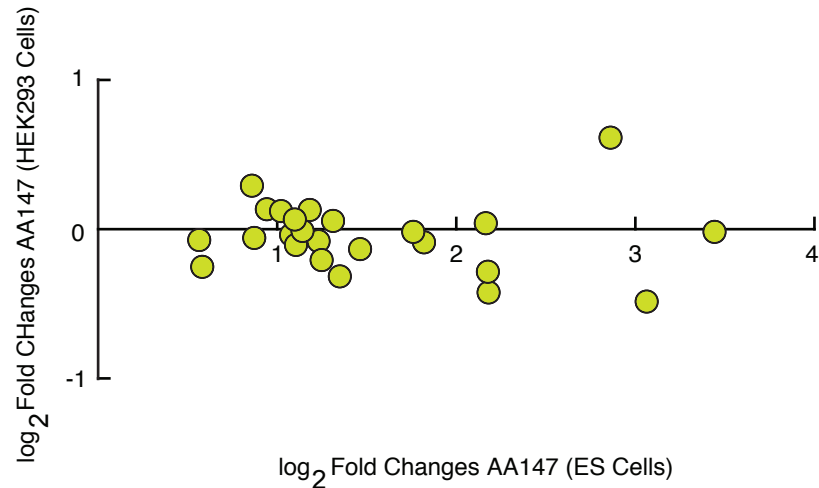


Figure S3. AA147 treatment does not induce mesodermal marker genes in HEK293 cells. The \log_2 fold changes of mesodermal marker genes identified in the RNA-Seq datasets after AA147 treatment (10 μ M)-of HEK293 cells are shown on the y-axis and are plotted against the \log_2 fold changes of AA147-treated (10 μ M) hESCs on the x-axis (37).

Table S1. Summary of genes used in volcano plots. Specific genes that were identified for the three lineages ectoderm, mesoderm, and endoderm as well as pluripotency markers, ATF6 target genes, and endothelia specific markers are summarized. Table is provided as a .xls file in the online supporting files.

Table S2. Raw RNA-seq data. The data collected for the RNA Seq analysis of hESC treated with 10 μ M AA147 or RP22 for 13 days are summarized. Three independent experimental repeats were performed and data were collected as reads per kilobase of transcript per million (RPKM) and are presented as AA147 gene expression levels relative to RP22 treated samples. Table is provided as a .xls file in the online supporting files.

Table S3. Comparison study using other cell types and tissues. RNA Seq data of differentiating hESC treated with 10 μ M AA147 or RP22 were collected as reads per kilobase of transcript per million (RPKM), followed by alignment with online available RNA Seq data sets to identify differential differences and/ or the generation of specific cell types or tissues upon AA147 treatment. Table is provided as a .xls file in the online supporting files.

Tissue or cell type	Accession code(s)
Adipose	ERR015534; ERR030888
Adrenal gland	ERR030889
B cells	SRR1613932; SRR805725; SRR805736; SRR805747; SRR805758; SRR805769
GM12878 B-lymphocyte cell line	SRR521466; SRR521467
GM12891 B-lymphocyte cell line	SRR521531; SRR521532; SRR521533
GM12892 B-lymphocyte cell line	SRR521534; SRR521535; SRR521536; SRR521537
Ramos B cell line	SRR023855; SRR023856
Bladder	SRR787270
Brain: whole	ERR030890; SRR787271; SRR309262
Brain: cerebellum	SRR306844; SRR306845; SRR306846
Brain: dorsolateral prefrontal cortex	SRR1047838; SRR1047843; SRR1047848; SRR1047853; SRR1047858
Brain: frontal lobe	SRR306838; SRR306839
Brain: hypothalamus	ERR015537
Brain: prefrontal cortex	SRR306840; SRR306841; SRR306842
Brain: temporal lobe	SRR306843
Breast	ERR030891; SRR787272
Breast tumor: benign	SRR791066; SRR791067; SRR791068; SRR791069; SRR791070; SRR791071; SRR791072; SRR791073
Breast tumor: ER positive	SRR791043; SRR791044; SRR791045; SRR791046; SRR791047; SRR791048; SRR791049; SRR791050
Breast tumor: Her2 positive	SRR791052; SRR791054; SRR791056; SRR791057; SRR791058; SRR791059; SRR791061; SRR791062
Breast tumor: triple negative	SRR791051; SRR791053; SRR791055; SRR791060; SRR791063; SRR791064; SRR791074
Caco-2 cells (colorectal adenocarcinoma cell line)	SRR927190
Colon	ERR30892; ERR015535; SRR787273
NHEK cells (epidermal keratinocytes)	SRR521509
Epidermis	SRR787281; SRR835999
Fibroblast: foreskin	SRR309269
Fibroblast: lung	SRR309267; SRR309268; SRR309270; SRR521527; SRR521528; SRR521529; SRR521530
Gastric tissue	SRR585570; SRR585571
Gastric tumor	SRR585572; SRR585573; SRR585574
SNU484 cells (gastric tumor cell line)	SRR585575
SNU601 cells (gastric tumor cell line)	SRR585576
SNU668 cells (gastric tumor cell line)	SRR585577
Granulocytes	SRR1613937
H1-hESC cells (human embryonic stem cells)	SRR521501; SRR521502
HCT-166 cells (colorectal carcinoma cell line)	SRR521538; SRR521539; SRR521540; SRR521541; SRR521542; SRR521543
Heart	ERR030894; ERR015536; SRR306847; SRR306848; SRR306849; SRR306850; SRR787274
HEK-293 cells (human embryonic kidney cell line)	SRR648667; SRR023853; SRR023854

HeLa cells (cervical adenocarcinoma cell line)	SRR309265; SRR521505; SRR521506
Hematopoietic stem and progenitor cells	SRR772114
HepG2 cells (hepatocellular carcinoma cell line)	SRR521507; SRR521508
HSMM cells (human skeletal muscle cells and myoblasts)	SRR521516; SRR521517; SRR521518; SRR521519
HUVEC cells (primary umbilical vein endothelial cells)	SRR521503; SRR521504
K562 cells (bone marrow lymphoblast cell line, from a patient with chronic myelogenous leukemia)	SRR521468; SRR521474; SRR521475
Kidney	ERR030893; ERR015538; SRR306851; SRR306852; SRR306853; SRR787275
Leukocyte	ERR030900
LHCN-M2 cells (immortalized skeletal myoblasts)	SRR521544; SRR521545; SRR521546
Endoderm (induced from embryonic stem cells)	SRR1036393
H7-hESC cells (human embryonic stem cells)	SRR1036391
Liver	ERR030895; ERR015539; SRR306854; SRR306855; SRR306856; SRR309264
Lung	ERR030896; ERR015540; SRR787277
Lymph node	ERR030897
MCF7 cells (breast metastatic adenocarcinoma cell line)	SRR521521; SRR521522; SRR521523; SRR521524; SRR521525; SRR521526
Monocytes	SRR1613933
Natural killer cells	SRR1613931
Ovary	ERR030901; ERR015541; SRR787279
Pancreatic islet cells	SRR957884; SRR957885; SRR957886; SRR957887; SRR957888; SRR957889
Placenta	SRR309266
Prostate	ERR030898; SRR787280
Retina	SRR548611
Skeletal muscle	ERR030899; ERR015542; SRR787278
Smooth muscle, airway	SRR1039508; SRR1039512
Spleen	ERR015543
T cells, memory	SRR1613934
T cells, naïve cytotoxic	SRR1613936
T cells, naïve helper	SRR1613935
Testis	ERR030902; ERR015544; SRR306857; SRR306858; SRR309263
Thyroid	ERR030903; SRR517615
This work:	
Stem cell, pre-treatment control (HUES9)	SRR6286138; SRR6286139; SRR6286140
Stem cells treated with AA147 (AA147)	SRR6286141; SRR6286142; SRR6286143
Stem cells treated with RP22 (RP22)	SRR6286144; SRR6286145; SRR6286146

Table S4. RNA-seq data set in our transcriptome database. Summary of tissues and cell types, including accession codes that were used to generate the tissue-correlation diagram shown in Figure 1F.